Deep Denoising Channel Extrapolation for IRS-Assisted OFDM Systems

Mubasher Ahmed Khan, Huijin Kang, Muhammad Awais and Yun Hee Kim
Department of Electronics and Information Convergence Engineering
Kyung Hee University, Korea
Email: {mubasher, gmldi118, mawais, yheekim}@khu.ac.kr.

***Abstract*—Intelligent reflecting surface (IRS) has emerged as a promising solution for future networks in improving the coverage and spectral efficiency by adapting its reflection pattern to the channel environments. To enable this, it is essential to acquire channel state information for which deep learning networks have been popularly applied recently. In this paper, we apply and optimize a deep denoising network to estimate the IRS-cascaded frequency selective fading channel with a reduced reflection pilot pattern for an IRS-enhanced orthogonal frequency division multiplexing system. The proposed network designed to support various noise levels with a single network model is shown to provide a reasonably good channel extrapolation performance when compared with the benchmark networks optimized for each noise level.**

***Index Terms*—Channel estimation, deep learning, intelligent reflecting surface, orthogonal frequency division multiplexing**

I. Introduction

Intelligent reflecting surfaces (IRSs) have drawn significant attention as a key technology for next-generation networks since it can boost spectral and energy efficiency while resolving signal blockage problems [1]. An IRS is made up of many passive reflecting elements that can artificially control the propagation of electromagnetic waves. By optimizing the reflection pattern, IRS-assisted wireless communications have been shown to enhance their communication quality without significantly increasing energy consumption or implementation costs [1], [2].

To fully utilize the benefits of a passive IRS, a large number of reflecting elements is required along with accurate channel state information (CSI). To obtain the CSI, the IRS cascaded channel from a device to a base station (BS) via an IRS has been estimated at the BS or device in general since a passive IRS incapable of performing signal processing cannot estimate the channels for itself. There exist some challenges in IRS cascaded channel estimation which are due to the non-Gaussian property of the IRS cascaded channel that renders the optimal minimum mean square error estimator intractable and due to the estimation of massive channel components associated with IRS elements. For the first challenge, deep learning networks have been applied to obtain an estimate close to the optimal one for IRS-cascaded channel estimation [3]. Channel estimation with a reduced pilot reflection pattern has been applied to tackle the second challenge [4], [5]. However, most studies have assumed frequency-flat fading in IRS-cascaded channel estimation.

In practice, wireless channels tend to be frequency selective multi-path fading for which orthogonal frequency division multiplexing (OFDM) is a natural choice [6]. Channel estimation for OFDM without IRS was studied with a deep residual network for super-resolution in the frequency domain [7]. Channel estimation for an IRS-assisted OFDM system was studied when the channel measurements are available for all IRS elements with the full pilot overhead [8]. To reduce the pilot overhead, a residual network (ResNet) was adopted and optimized for IRS-assisted OFDM to provide spatial-domain super-resolution with the channel measurements made only for part of the IRS elements [9]. However, ResNet was optimized for each signal-to-noise power ratio (SNR) value, which needs extensive training data and training time as well as extensive memories to save the model parameters optimized for each SNR value [9].

To cope with the drawbacks of ResNet, we address the modified deep residual U-shaped network (mDRUNet) proposed for IRS channel estimation in flat fading [5] to OFDM-based IRS cascaded channel estimation. The network employs a noise map at the input to develop a single trained network dealing with various SNR values, which can reduce the offline training overhead and hardware costs significantly.

II. System and Channel Models

We consider an IRS assisted OFDM system experiencing multi-path fading channels as depicted in Fig. 1. A BS and a device are equipped with a single antenna for each, and a passive IRS is constructed with N reflecting elements. The channel impulse response (CIR) between the BS and IRS, denoted by $\mathbf{g}(\tau)$, and the CIR between the IRS and device, denoted by $\mathbf{f}(\tau)$, are modelled as

$$\mathbf{g}(\tau) = \sum_{l=1}^{L_g} \alpha_l^g \mathbf{a}^*(\theta_l^g, \psi_l^g)\delta(\tau - \tau_l^g), \quad (1)$$

$$\mathbf{f}(\tau) = \sum_{l=1}^{L_f} \alpha_l^f \mathbf{a}^*(\theta_l^f, \psi_l^f)\delta(\tau - \tau_l^f), \quad (2)$$

where L_g (L_f) is the number of multi-paths in CIR $\mathbf{g}(\tau)$ ($\mathbf{f}(\tau)$), α_l^x, τ_l^x, θ_l^x, and ψ_l^x represent the complex fading amplitude, delay time, azimuth angle, and elevation angle of the lth

This research was supported by the National Research Foundation of Korea (NRF) under Grant NRF-2021R1A2C1005869 and by the Institute of Information & Communications Technology Planning & Evaluation (IITP) under the Information Technology Research Center (ITRC) support program IITP-2023-2021-0-02046, with funding from the Ministry of Science and ICT (MSIT), Korea.

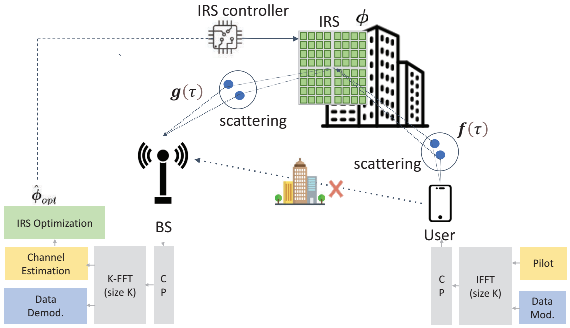

Fig. 1. System model for an IRS-assisted OFDM communication network.

path in CIR $x \in \{g, f\}$, respectively, and $\mathbf{a}(\theta, \psi) \in \mathbb{C}^{N\times 1}$ is the array response of the IRS employing the $N_h \times N_v$ uniform planar array. Specifically, we have

$$\mathbf{a}(\theta, \psi) = \tilde{\mathbf{a}}(u, v)|_{u=\sin(\theta)\cos(\psi), v=\sin(\psi)} \tag{3}$$

with $\tilde{\mathbf{a}}(u, v) = \tilde{\mathbf{a}}_{N_h}(u) \otimes \tilde{\mathbf{a}}_{N_v}(v)$, where $\otimes$ is the Kronecker product and

$$\tilde{\mathbf{a}}_J(x) = [1, e^{-j2\pi\frac{d}{\lambda}x}, \cdots, e^{-j2\pi\frac{d}{\lambda}(J-1)x}]^T \tag{4}$$

is the array response of a uniform linear array with J elements at spacing $d = \lambda/2$ for a signal of wavelength λ incident with angular parameter x. Accordingly, the IRS cascaded channel is described as

$$\mathbf{h}(\tau) = \sum_{l=1}^{L_h} \alpha_l^h \tilde{\mathbf{a}}(u_l^h, v_l^h)\delta(\tau - \tau_l^h) = \sum_{l=1}^{L_h} \mathbf{h}_l \delta(\tau - \Delta_l^h T_s), \tag{5}$$

where $L_h = L_g L_f$, $\alpha_l^h = \alpha_{l_1}^g \alpha_{l_2}^f$, $\tau_l^h = \tau_{l_1}^g + \tau_{l_2}^f = \Delta_l^h T_s$ with sampling time T_s, and $\mathbf{h}_l = \alpha_l^h \tilde{\mathbf{a}}(u_l^h, v_l^h)$ with $u_l^h = -\sin(\theta_{l_1}^g)\cos(\psi_{l_1}^g) + \sin(\theta_{l_2}^f)\cos(\psi_{l_2}^f)$ and $v_l^h = -\cos(\psi_{l_1}^g) + \cos(\psi_{l_2}^f)$ for $l = (l_1 - 1)L_f + l_2$ with $l_1 = 1, 2, \cdots, L_g$ and $l_2 = 1, 2, \cdots, L_f$.

To estimate the multi-path fading channel, the device transmits the OFDM symbol generated with fast Fourier transform (FFT) of size K during the channel estimation phase. The frequency-domain symbol vector constructing the tth OFDM symbol is denoted by $\mathbf{X}_t = [X_t[0], X_t[1], \cdots, X_t[K-1]]^T$ for $t = 1, 2, \cdots, T_P$, where $X_t[k]$ is the pilot symbol at kth subcarrier and T_P is the number of pilot OFDM symbols. The IRS reflects the tth OFDM symbol with reflection pattern $\boldsymbol{\phi}_t = [\phi_{t1}, \phi_{t2}, \cdots, \phi_{tN}]^T$. To reduce the pilot overhead, only a subset of IRS elements are turned on at each symbol time as $|\phi_{tn}| = 1$ for $n \in \mathcal{N}_{on}$ and $\phi_{tn} = 0$ for $n \in \mathcal{N}_{on}^c$, where $\mathcal{N}_{on}$ is the set of IRS elements turned on to reflect a signal.

The received symbol of the kth subcarrier at the BS is expressed as

$$Y_t[k] = \boldsymbol{\phi}_t^T \mathbf{H}[k] X_t[k] + W_t[k], \ k = 0, 1, ..., K-1, \tag{6}$$

where $W_t[k] \sim \mathcal{CN}(0, \sigma^2)$ is the zero-mean complex Gaussian noise with variance σ^2 at the kth subcarrier and $\mathbf{H}[k] \in \mathbb{C}^{N\times 1}$ is the channel frequency response (CFR) of the cascaded channel at the kth subcarrier. The CFR is expressed as

$$\mathbf{H}[k] = \sum_{l=1}^{L_k} \alpha_l^h \tilde{\mathbf{a}}(\vartheta_l^h, \varphi_l^h) e^{-j2\pi k \Delta_l^h / K} = \mathbf{G}[k] \circ \mathbf{F}[k], \tag{7}$$

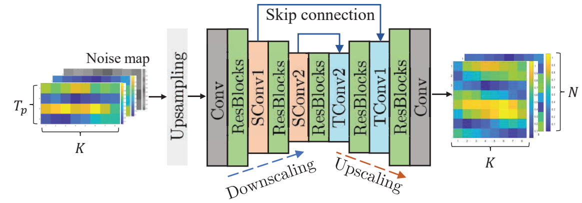

Fig. 2. mDRUNET structure for channel extrapolation.

where $\mathbf{G}[k]$ and $\mathbf{F}[k]$ represent the CFR of $\mathbf{g}(\tau)$ and $\mathbf{f}(\tau)$, respectively, and $\circ$ denotes the Hadamard multiplication. All the received symbols during the channel estimation phase are expressed in a vector form as

$$\mathbf{Y}[k] = [Y_1[k], Y_2[k], ..., Y_{T_P}[k]]^T = \mathbf{\Phi}_P \mathbf{H}[k] + \mathbf{W}[k], \tag{8}$$

where $\mathbf{\Phi}_P = [\phi_1, \phi_2, \cdots, \phi_{T_P}]^T$ and $\mathbf{W}[k] = [W_1[k], W_2[k], \cdots, W_{T_P}[k]]^T$.

III. Deep Denoising Channel Extrapolation

This section describes the data preparation and network model for deep-learning based channel estimation. For the input data, we adopt the $T_P \times T_P$ orthogonal matrix subject to $|[\mathbf{\Xi}]_{ij}| = 1$ and $\mathbf{\Xi}\mathbf{\Xi}^H = \mathbf{\Xi}^H\mathbf{\Xi} = T_P \mathbf{I}_{T_P}$ for a subset of IRS elements turned on for reflection. Then, we can express $\mathbf{\Phi}_P = \mathbf{\Xi}\mathbf{B}$, where $\mathbf{B} \in \mathbb{R}^{T_P \times N}$ is the reflection pattern matching matrix given by $[\mathbf{B}]_{mn} = 1$ for $n \in \mathcal{N}_{on}$ and $[\mathbf{B}]_{mn} = 0$ for $n \notin \mathcal{N}_{on}$. Then, the received signal (8) can be expressed as

$$\mathbf{Y}[k] = \mathbf{\Xi}\mathbf{B}\mathbf{H}[k] + \mathbf{W}[k] = \mathbf{\Xi}\mathbf{H}^{\mathcal{P}}[k] + \mathbf{W}[k], \tag{9}$$

where $\mathbf{H}^{\mathcal{P}}[k] = \mathbf{B}\mathbf{H}[k] \in \mathbb{C}^{T_P \times 1}$ represents a subset of the IRS cascaded channels observed at the receiver for the IRS elements used in channel estimation at the kth subcarrier. The least-square (LS) estimation of the punctured CFR can be computed as

$$\hat{\mathbf{H}}_{\text{ls}}^{\mathcal{P}}[k] = (\mathbf{\Xi}^H\mathbf{\Xi})^{-1}\mathbf{\Xi}^H \mathbf{Y}[k] = \mathbf{H}^{\mathcal{P}}[k] + \mathbf{W}_{\text{ls}}[k], \tag{10}$$

where $\mathbf{W}_{\text{ls}}[k] \sim \mathcal{CN}(\mathbf{0}, \sigma_{\text{ls}}^2, \mathbf{I}_{T_P})$ and $\sigma_{\text{ls}}^2 = \sigma^2/T_P$ is the noise variance of the LS estimate.

With the LS estimates $\hat{\mathbf{H}}_{\text{ls}}^{\mathcal{P}}[k]\}_{k=0}^{K-1}$ on the punctured CFR, we obtain the estimate $\{\hat{\mathbf{H}}[k]\}_{k=0}^{K-1}$ of the original CFR $\{\mathbf{H}[k]\}_{k=0}^{K-1}$ by modifying the mDRUNet proposed in [5] as shown in Fig.2. The input is constructed by $T_P \times K \times 3$, where the first two channels of size $T_P \times K$ are the real and imaginary parts of $\{\hat{\mathbf{H}}_{\text{ls}}^{\mathcal{P}}[k]\}_{k=0}^{K-1}$ whilst the third channel of size $T_P \times K$ is given by the noise variance $\sigma_{\text{ls}}^2/2$ of the real and imaginary parts of the LS estimate. The three channels are upsampled to obtain the $N \times K \times 3$ input by duplicating the LS estimates and variances. The output is given by the real and imaginary parts of the extrapolated channel $\{\hat{\mathbf{H}}[k]\}_{k=0}^{K-1}$ of size $T_P \times K \times 2$. Here, the noise variance in the input allows us to train a single unified model that handles diverse noise levels. The DRUNet is constructed by the two-dimensional convolutional network (Conv) followed by residual blocks (ResBlock) and two scaling connected by

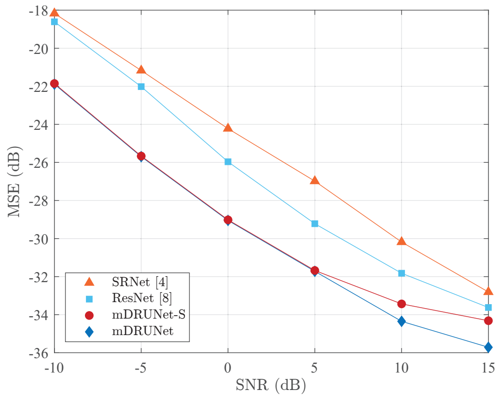

Fig. 3. MSE of the cascaded IRS-OFDM channel as the channel SNR increases when $T_P = 32$ with 50 % pilot overhead reduction.

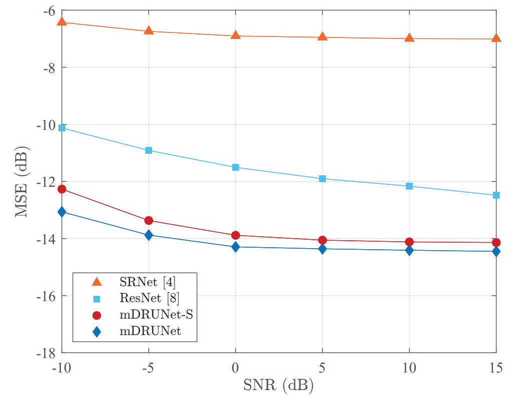

Fig. 4. MSE of the cascaded IRS-OFDM channel as the channel SNR increases when and $T_P = 16$ with 25 % pilot overhead reduction..

an identity skip for each scaling consisting of the downscaling operation involving a 2×2 strided convolution (SConv) and the subsequent upscaling operation employing a 2×2 transposed convolution (TConv). The last scaling is connected to the convolutional layer to provide the output. The number of channels at Conv, SConv1 (TConv1) and SConv2 (TConv2) are 64, 128, and 256, respectively, where the activation functions are not employed. Each ResBlock consists of two successive residual blocks accompanied by ReLU activation function at the end of each block. The model parameters $\mathbf{\Theta}$ of the mDRUNet with the output described by $f(\{\hat{\mathbf{H}}_{\text{ls}}^{\mathcal{P}}[k]\}_{k=0}^{K-1}, \sigma_{\text{ls}}^2; \mathbf{\Theta})$ with input $(\{\hat{\mathbf{H}}_{\text{ls}}^{\mathcal{P}}\}_{k=0}^{K-1}, \sigma_{\text{ls}}^2)$ is trained to minimize the mean square error (MSE) loss function.

IV. Experimental Results

To evaluate the performance, we adopt $N = 8 \times 8 = 64$ for the IRS and $K = 64$ for the FFT size when the location of the BS, IRS, and device in the (x, y, z) coordinates is given by $(0, 0, 10)$, $(50, 50, 10)$, and $(60, 40, 0)$ in meters, respectively. The multipath intensity profile of the channels is set to the uniform power with $L_g = L_f = 2$ at the delay of $[\tau_1^g, \tau_2^g] = [0, 1]$ and $[\tau_1^f, \tau_2^f] = [0, 2]$ and the azimuth and elevations angles are generated from the uniform distribution over $[-\Delta\frac{\pi}{2}, \Delta\frac{\pi}{2})$ with the normalized maximum angular spread $\Delta = 0.1$. We generate total D data samples that are allocated to training, validation, and testing at $8 : 1 : 1$ ratio. For training, the ADAM optimizer of learning rate 10^{-3} is used with batch size 100 up to 100 epochs. The benchmark schemes are optimized for each SNR value with $D = 100$k data samples whilst the proposed mDRUNet is optimized for various SNR levels with D data samples having different SNR values.

Figs. 3 and 4 provide the normalized MSE of the deep-learning based estimators as the channel SNR, $1/\sigma^2$, varies when $T_P = 32$ and $T_P = 16$, respectively, corresponding to the pilot overhead reduction by 50 % and 25 % when compared to the full reflection. Here, mDRUNet-S denotes mDRUNet with a single network trained over all SNR values while mDRUNet, SRNet, and ResNet denote mDRUNet, super-resolution network [4], and ResNet [9] optimized for each SNR value, respectively. The results show that mDRUNet provides a significant performance improvement compared to SRNet [4] and ResNet [9]. Furthermore, mDRUNet-S deploying a single model for all SNR values exhibits a negligible loss when compared to mDRUNet optimized for each SNR value, which alleviates the training burden in data size and delay.

V. Concluding Remarks

This paper presented a robust deep-learning based channel extrapolation method for the IRS-cascaded OFDM system by utilizing the noise variance input additionally. The results showed that the proposed mDRUNet with a single trained network provides a much better performance than the benchmarks whilst simultaneously reducing the training data and training time.

References

[1] C. Huang, A. Zappone, G. C. Alexandropoulos, M. Debbah and C. Yuen, "Reconfigurable intelligent surfaces for energy efficiency in wireless communication," *IEEE Trans. Wireless. Commun.*, vol. 18, no. 8, pp. 4157-4170, Aug. 2019.

[2] Q. Wu and R. Zhang, "Towards smart and reconfigurable environment: Intelligent reflecting surface aided wireless network," *IEEE Commun. Mag.*., vol. 58, no. 1, pp. 106-112, Jan 2020.

[3] N. K. Kundu and M. R. McKay, "Channel estimation for reconfigurable intelligent surface aided MISO communications: From LMMSE to deep learning solutions." *IEEE Open J. Commun. Soc.*, vol. 2, pp. 471-487, 2021.

[4] S. Yin, Y. Li, Y. Tian and F. R. Yu, "Intelligent reflecting surface enhanced wireless communications with deep-learning-based channel prediction," *IEEE Trans. Veh. Technol.*., vol. 71, no. 1, pp. 1049-1053, Jan. 2022.

[5] M. Awais, M. A. Khan and Y. H. Kim, "Deep denoising and unfolding for IRS cascaded channel estimation with element-grouping," *IEEE Wireless. Commun. Lett.*, early access, doi: 10.1109/LWC.2023.3290204.

[6] Y. Yang, B. Zheng, S. Zhang and R. Zhang, "Intelligent reflecting surface meets OFDM: protocol design and rate maximization," *IEEE Trans. Commun.*, vol. 68, no. 7, pp. 4522-4535, Jul. 2020.

[7] L. Li, H. Chen, H. -H. Chang and L. Liu, "Deep residual learning meets OFDM channel estimation," *IEEE Wireless. Commun. Lett.*, vol. 9, pp. 615–618, May 2020.

[8] S. Liu, Z. Gao, J. Zhang, M. Di Renzo and M.-S. Alouini, "Deep denoising neural network assisted compressive channel estimation for mmWave intelligent reflecting surfaces," *IEEE Trans. Veh. Technol.*, vol. 69, no. 8, pp. 9223-9228, Aug. 2020.

[9] H. Kang, S. Oh, S. Cho and Y. H. Kim, "Deep learning based channel prediction for IRS assisted OFDM systems," *Proc. KICS Summer Conf.*, Jeju, Korea, Jun. 2023.